

Numerical Studies on the Effectiveness of Dynamic Compaction in Loose Granular Deposits Using Shear Wave Velocity Profiling

Saptarshi Kundu¹ · B. V. S. Viswanadham¹

Received: 14 May 2017 / Accepted: 7 February 2018 / Published online: 12 March 2018
© Indian Geotechnical Society 2018

Abstract Over the past few decades, Dynamic compaction (DC) has gained popularity as an effective improvement technique for geomaterials in view of its simplicity, low-environmental impact and cost effectiveness. The low carbon footprint associated with this ground remediation method addresses the adverse ecological threats imposed on the environment and society due to unsustainable geotechnical engineering practices encountered in the face of rapid urbanization. In the literature, studies related to numerical modelling of DC are limited, and the existing databases are founded on field trials, past experience and empirical equations. Further, till date, numerical evaluation of improvement in soil strength post DC is restricted primarily to change in relative density of soil samples before and after impact, whereas, in the field, shear wave velocity (V_s) profiling is frequently adopted as a monitoring technique for measuring the degree and depth of improvement. This necessitates a quantitative correlation between the DC design parameters (tamper radius, energy and momentum) and the available shear wave profile data measured in the field for effective design and execution of DC methodology. In order to overcome the above mentioned research gaps, an elasto-plastic soil model with Drucker–Prager failure criteria is incorporated in the present study using FE software ABAQUS. The response of the soil model to large strains developed during multiple tamper drops on dry sand is investigated numerically, and validated with the results

of a centrifuge model test, and numerical analyses published in literature. Further, the shear wave velocity of soil samples is assessed numerically based on the value of shear modulus, and subsequent improvement in model soil due to impact (66% in the present case) is studied to arrive at a better practical application. The results are compared with physically observed field data, and are found to corroborate well. Subsequent parametric studies are carried out by varying the design parameters related to DC, which indicates that the degree and depth of improvement of soil in terms of V_s increases substantially (about 40%) with an increase in momentum and decreasing tamper radius (about 60%), whereas, energy imparted has comparatively lesser impact on improvement. A method is eventually proposed with design equations to calculate the improvement after DC in field based on V_s profiling, depending on momentum and radius of tamper. Further, structural requirements coupled with V_s profile data computed in the ground remediated by DC can help in avoiding construction of expensive deep foundations in sites exhibiting poor subsoil profiles, thereby economizing the project. In addition, the above concept ensures sustainability in engineering practices by enabling land-reclamation and utilization of sites exhibiting locally available compressible soils for infrastructure construction and foundation support.

Keywords FE modelling · ABAQUS · Dynamic compaction · Shear wave velocity

✉ Saptarshi Kundu
kundusaptarshi@iitb.ac.in; saptarshikundu123@gmail.com

B. V. S. Viswanadham
viswam@civil.iitb.ac.in

¹ Department of Civil Engineering, Indian Institute of Technology Bombay, Powai, Mumbai 400076, India

Introduction

Over the past few years, rapid urbanization and demand for new infrastructures have aroused discussions in various political, social and economic arenas on the increasing

carbon dioxide emission levels associated with the construction industry. Thus, the necessity of sustainable environment-friendly construction methodologies has come to the forefront, especially in connection with foundation design on loose subsoils, along with due consideration of quality control and cost involved. In recent years, dynamic compaction (DC) has evolved as a widely adopted ground remediation technique for improving the characteristics of loose cohesionless soils by the transmission of high-energy waves within the soil mass. In addition to being economically viable, the carbon footprint associated with DC (both for direct and indirect emissions) is significantly less when compared to conventional deep foundation techniques [1]. Hence, substantial reduction of greenhouse gas (GHG) emissions occur in association with this technology, thereby addressing the unsustainable ecological imbalance inflicted by alternate geotechnical engineering operations.

The current practice for evaluating the feasibility of DC and optimization related to desired depth and degree of improvement in the field are not properly established. The decisions of proper selection of operational parameters (viz. mass, height of fall, energy, tamper radius etc.) have to be made depending primarily on field trials, past experience, and empirical formulas suggested by Menard and Broise [2] and Leonards et al. [3]. In the literature, field tests and case studies on the use of DC in field were documented by Mayne et al. [4], Kumar and Puri [5], Zou et al. [6], Bo et al. [7] and Feng et al. [8]. However, limited information can be gathered from the field studies mentioned above due to difficulties encountered on account of heterogeneous soil at the site, and problems related to instrumentation and data acquisition. Moreover, the results presented were extremely site-specific, and cannot be generalized for effective modelling of DC in the field. Further, laboratory investigations on low energy compaction process were carried out by Feng et al. [9], Arslan et al. [10], Hajjalilue-Bonab and Rezaei [11], Bonab and Zare [12] and Kundu and Viswanadham [13]. However, 1 g conditions cannot replicate stress history and state of stress accurately in model as that existing in a full-scale prototype [14]. Hence, stresses and deformations obtained on the basis of the laboratory investigations conducted at 1 g cannot predict the actual soil response in the field.

As an alternative approach, researchers like Scott and Pearce [15], Holeyman [16], Smits and Quelerij [17], Chow et al. [18–20], Corapcioglu et al. [21], Gunaratne et al. [22] and Pan and Selby [23] modelled the impact of DC on geomaterials analytically and/or numerically. However, most of the studies were based on one-dimensional soil models or elastic constitutive laws, which beside other shortcomings, could not simulate the lateral spreading taking place during ground improvement. Further, in

the advanced numerical soil models used by Gu and Lee [24] and Ghassemi et al. [25], the improvement in soil strength post DC was analyzed with respect to change in relative density of soil samples before and after impact, whereas, in actual practise, CPT or SASW techniques are more frequently adopted in field to monitor the soil improvement after ground remediation techniques. Another notable factor is that, the initial relative density in case of Gu and Lee [24] and initial SPT value in case of Nashed et al. [26] were assumed to be constant with depth, contrary to actual field condition. Thus, there is a possibility that the predicted values related to depth and degree of improvement may not represent the results obtained in field during soil investigation post DC.

In the present paper, an attempt is made to address the above research gaps by numerical investigations related to ground response during DC at a single point, and subsequently study the intrinsic design parameters affecting the degree and extent of improvement. The constitutive law and modelling considerations involved are discussed in detail, and a validation check has been conducted by comparing the analysis results with relative density measurements reported by Oshima and Takada [27] during centrifuge model tests related to DC of dry sand. In addition, the stress paths obtained in the present study are compared with the numerical model predictions of Gu and Lee [24], indicating a close correlation. Further, the shear wave velocity of soil samples before and after impact is assessed numerically based on the value of shear modulus, and subsequent improvement in loose soils post DC is investigated by means of shear wave profiling. SASW technique is selected in the present study owing to its non-invasive nature, and its ability to overcome the logistic effort of drilling expensive boreholes or inserting probes in the field, which are associated with other subsoil investigation techniques like SPT and CPT, especially in the present-day context of intensely urbanized settings. The results obtained have been compared with observed field data, and are found to corroborate well. Finally, the effect of energy, momentum and tamper base area on the depth and degree of improvement due to DC are modelled and examined.

Modelling Considerations for DC

Meshing Details and Constitutive Law

The model mesh developed in ABAQUS for the present study related to DC is shown in Fig. 1. It represents an axisymmetric model consisting of a tamper mass of radius r (AEFG) and a soil body of width R and depth D (ABCD). Line DAG represents the axis of symmetry. Both the soil and the tamper mass are modelled with bilinear

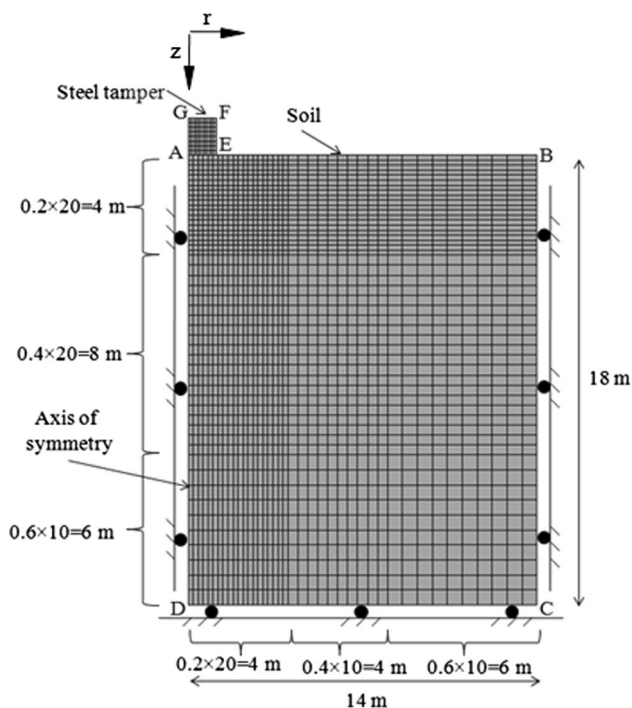


Fig. 1 Two-dimensional axisymmetric FE model mesh

axisymmetric isoparametric elements. Further, at each node of the axisymmetric elements used in meshing, two degrees of freedom, namely u and w (in radial and vertical direction respectively) are defined related to displacement of soil mass under dynamic impact. The mesh size in the present study is selected in accordance with the findings of Zerwer et al. [28], wherein use of very small element size was found to generate numerical instability, whereas, larger elements restricted movement of shorter waves associated with higher frequencies. In view of the above, the soil mass close to the tamper is modelled with finer elements as compared to points located away from the impact zone to ensure numerical accuracy. Accordingly, an element size of 0.2 by 0.2 m is used close to zone of impact for accurate modelling of deformations and stresses, whereas, away from the point of impact, the mesh size is increased to 0.6 by 0.6 m. The interaction between soil and tamper mass is modelled using contact interaction scheme in ABAQUS involving both tangential and normal components. The interaction component in the normal direction is assumed to be hard with separation option activated. Further, a friction coefficient of 0.2 is assumed in the analysis based on standard frictional values registered between steel mass (tamper in this case) and soil surface. The tamper is modelled as an elastic material, having an elastic modulus of 210 GPa and Poisson’s ratio of 0.303 as observed in case of standard steel.

The soil is modelled as an elasto-plastic material with an associative flow rule, and the plastic behaviour of soil is

simulated by using the constitutive law proposed by Dimaggio and Sandler [29] and subsequently used by Gu and Lee [24] for replicating large-strain dynamic formulation using 2D FE analysis. The above mentioned constitutive model is well suited for predicting the response of soil to DC, wherein pressure dependent yielding occurs in association with large strains in the vicinity of tamper mass. It involves prediction using a yield surface (refer Fig. 2) comprising of a shear failure surface (line AB) represented by f_s in Eq. (1) and a hardening cap (ellipse BC) represented by f_h in Eq. (2):

$$f_s = \sqrt{J_{2D}} - \alpha I_1 - \kappa = 0 \tag{1}$$

$$f_h = (I_1 - l)^2 + R^2 J_{2D} - (x - l)^2 = 0 \tag{2}$$

where J_{2D} is second invariant of deviatoric stress, I_1 is first invariant of stress, α , κ and R are soil parameters, and parameter l is evaluated from Eq. (3) as follows:

$$l = \frac{x - R.\kappa}{1 + R.\alpha} \tag{3}$$

In the above equation, x is the hardening parameter which is related to plastic volumetric strain ϵ_v^p by Eq. (4):

$$x = -\frac{1}{D} \ln\left(1 - \frac{\epsilon_v^p}{W}\right) + x_o \tag{4}$$

In Eq. (4), D and W are soil parameters and x_o is the initial value of the hardening parameter. The position of the hardening cap is controlled by parameter x . Hence, as the soil is compacted, the plastic volumetric strain increases and so does the value of x to x' , x'' as shown in Fig. 2, implying that the hardening cap increases in size with progress of compaction. Further, the behaviour of soil, within the yield surface, is modelled as a non-linear elastic material using Poisson’s ratio and bulk modulus as presented in Eq. (5):

$$K = \frac{Vp'}{\kappa} \tag{5}$$

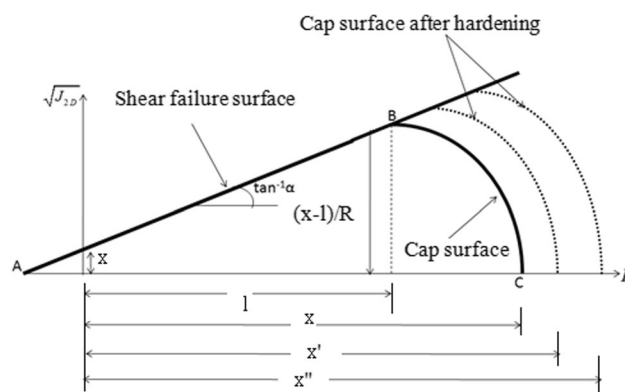


Fig. 2 Yield locus in $I_1 - \sqrt{J_{2D}}$ plane after hardening

where V is specific volume of soil, p' is mean stress and κ is the slope of the unloading line in the e - $\log p'$ curve. Equation (5) hereby takes into account the variation of elastic properties of soil with depth due to inclusion of the mean stress component (p'), which increases steadily with confinement. Thus, the soil properties selected in the present study replicate heterogeneities along the depth of soil mass, as commonly encountered in the field deposits. However, the present study being based on numerical simulations has inherent limitations related to accurate replication of heterogeneities encountered in the field, which is beyond the present research context. The constitutive law described above is not in-built in ABAQUS. Hence, user-defined subroutines are coded in FORTRAN programming language and fed as input in the present numerical simulation study.

Modelling of Tamping and Simulation of DC Process

The phenomena of falling of tamper mass on the soil surface has to be modelled as a dynamic process, wherein the tamper mass is released from the required drop height under gravity as shown in Fig. 3. There are different ways in which it can be achieved. The method adopted by majority of researchers was to release the tamper mass from a desired drop height so as to strike the soil surface with an impact velocity gained due to the height of fall. Another approach is to directly apply the impact velocity of the mass as the impact velocity calculated using Newton's laws of motion from Eq. (6):

$$V_0 = \sqrt{2gh} \quad (6)$$

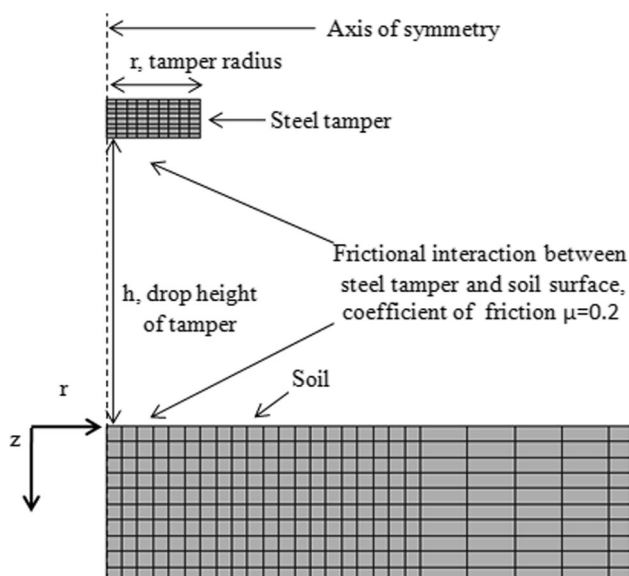


Fig. 3 Modelling scheme of DC with falling tamper mass

where, V_0 is the tamper velocity at the moment of impact, h represents the drop height and g is the ground acceleration ($= 9.81 \text{ m/sec}^2$).

The procedures followed sequentially to evolve at the technique of modelling DC numerically are discussed herein. In the initial step, in situ stresses at rest condition (referred to as geostatic stresses) are modelled and induced in the soil mass. The vertical stress is calculated by multiplying unit weight of soil with depth and lateral earth pressure is calculated by multiplying coefficient of lateral earth pressure ($k_0 = 0.5$ for all analysis in present study) with the computed vertical stress. In the first step, gravity load is applied so as to achieve a state of equilibrium with existing geostatic stresses at zero deformations. In the subsequent steps, repeated tamper impacts are modelled by directly applying the impact velocity to the mass at regular intervals. Due to large deformations involved in DC, an Updated Lagrangian formulation is used in the present study.

Validation with Published Results

The numerical model developed in ABAQUS is first validated with results of published literature to ensure its correctness and robustness. For the purpose of validation, the centrifuge test results reported by Oshima and Takada [27] and numerical analysis results of Gu and Lee [24] are selected. In the centrifuge experiment on DC conducted by Oshima and Takada [27], a prototype mass of 20 tonnes with base area of 4 m^2 was dropped repeatedly (40 times) from a drop height of 20 m. The same was modelled numerically by Gu and Lee [24], wherein a mass of 20 tonnes and base area of 3.98 m^2 was dropped with initial velocity of 19.81 m/sec successively (15 times), corresponding to a height of 20 m. In the present study, the soil properties for validation and subsequent analyses are assumed identical to that of the model soil used by Oshima and Takada [27], which essentially represents a field deposit. The relevant parameters for the constitutive law used in the analysis are presented in Table 1. Other material properties including Rayleigh damping coefficients, boundary conditions, mesh properties and DC parameters are kept identical to the numerical research work conducted by Gu and Lee [24] based on the centrifuge model parameters of Oshima and Takada [27]. The validation is performed with regard to two aspects, viz. by monitoring the change in relative density post impact and the stress paths generated in the process with increasing impacts.

Table 1 Material parameters adopted in present numerical analysis

Properties Soil type	D (m ² /kN)	W	R	α	κ (kPa)	κ_e	ν	RD (%)	Density (kN/m ³)
^a Sand	0.00018	0.4	4.33	0.231	0	0.003	0.3	35	14.70

^aProperties of Oshima and Takada [27] soil sample derived by Gu and Lee [24] which has been used subsequently in the validation study; D, W, R, α , κ : soil parameters adopted in elasto-plastic constitutive law; α , κ : Drucker–Prager parameters; κ_e : slope of e-log p curve used in prediction of bulk modulus of soil; ν : Poisson’s ratio and RD: relative density of soil

Validation of Change in Relative Density After DC

Figure 4a compares the variation of relative density with depth after DC corresponding to results reported by

Oshima and Takada [27], Gu and Lee [24] and that obtained in the present study. The contour lines corresponding to increase in relative density by 5, 10, 20 and 40% monitored after 15 impacts are presented in Fig. 4a, which correspond to final relative density values of 40, 45, 55 and 75% respectively in the improved soil stratum for an initial relative density of 35%. Further increase in relative density values beyond 75% is encountered in the soil model at shallower depths, but has not been presented in the context of the present validation analysis. From Fig. 4a, it can be inferred that, the vertical depth of improvement obtained in the present study have similar trends as that reported in previous studies, including the numerical simulation results of Gu and Lee [24]. However, some deviation can be observed for the contour lines in lateral direction, within the limits of numerical and experimental accuracy. Overall, it can be observed that the results of the present numerical analysis have corroborated with physically observed centrifuge test results, thereby validating the present FE model.

Validation of Stress Path Contours with Increasing Impacts

The stress changes in soil mass generated during dynamic impact using the present FEM model in ABAQUS for a point 2.0 m below the surface of the soil, 0.1 m away from the centreline are plotted in Fig. 4b. The stress paths obtained in the present study corresponding to 1st and 3rd impacts are shown, along with the results reported by Gu and Lee [24]. The similarity in orientations and magnitude of the stress path between the present study and those obtained by Gu and Lee [24] proves that the present modelling of DC is accurate and can be used for further parametric studies involving different field conditions. In this regard, it should be mentioned that the marginal variation between the numerical results reported by Gu and Lee [24] and those obtained in the present study may be attributed to differences in tolerance limits and number of iteration steps involved in both the cases.

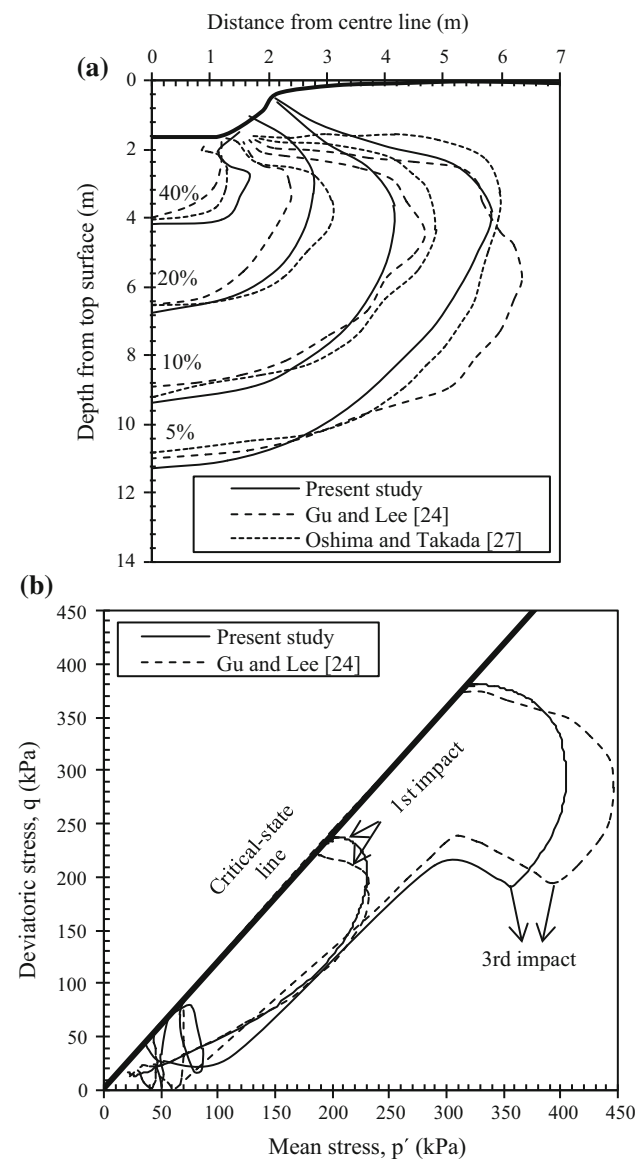


Fig. 4 Validation of developed DC numerical model with published literature. **a** Contour lines for increase in relative density after 15 impacts. **b** Stress path for soil (2 m below surface and 0.1 m from centreline) with increasing impacts as developed in the present study

Validation of Shear Wave Velocity Profile with Field Data

Subsoil investigation techniques like SASW are frequently adopted in field to monitor the state of soil existing at the site in terms of shear wave velocity data. The same technique holds good for monitoring the soil improvement before and after DC in field, wherein SASW is used frequently, as pointed out by Feng et al. [8]. The primary advantage of SASW technique lies in its non-intrusive nature, and its ability to cover soil investigation of large expanse of field area in very short span of time. Hence, in the present study, the soil improvement after DC is quantified using shear wave velocity measurements (V_s). The most common method of evaluating the shear modulus (G) is by conducting SASW, which accurately predicts the elastic moduli. However, a major problem encountered in this connection is to predict numerically the field dispersion curve (especially in case of layered soils exhibiting vertical and horizontal heterogeneities), inversion of which yields the shear wave velocity profile. Hence, in the present study, shear wave velocity profiling is calculated using the shear modulus (G) and density of soil (ρ) as presented in Eq. (7a). Further, the value of shear modulus (G) at any point is calculated using the standard relationship involving the bulk modulus (K), a parameter of the constitutive law used in the present study, [refer Eq. (5)] and Poisson's ratio (ν) as shown in Eq. (7b).

$$V_s = \sqrt{\frac{G}{\rho}} \quad (7a)$$

$$G = \frac{3K(1 - 2\nu)}{2(1 + \nu)} \quad (7b)$$

Earlier research in this area was restricted primarily to measurement of soil improvement at various depths along the center of tamper mass. However, as the improvement of soil after DC is maximum at the tamper center and reduces with increase in distance from the center, such a case can over-estimate the improvement. In the field, the optimum print spacing is generally chosen as 2 times the tamper diameter as per the database compiled by Chow et al. [20] on the basis of case histories of several DC project reports. This implies that the farthest point from center of impact is at a distance of 2 times the radius of tamper. Hence, in the present study, the improvement is observed by plotting the shear wave velocity (V_s) at a distance of 2 times the radius of tamper from tamper center. The corresponding results obtained are presented in Fig. 5. As evident from Fig. 5, there exists a good corroboration between the numerically computed (V_s) and field data measured by Feng et al. [8]. The slight deviation may be attributed to the fact that, in the present case, model soil properties of Oshima and

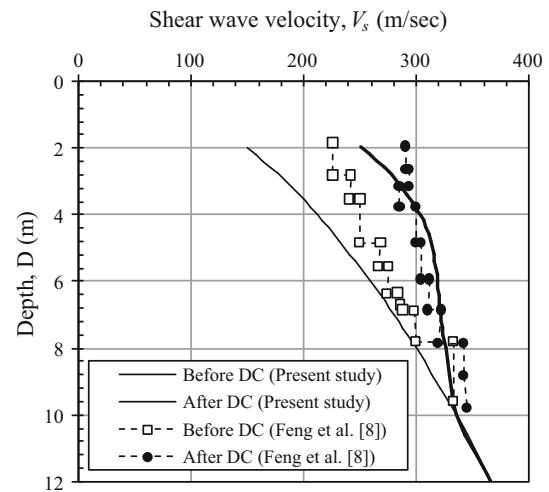


Fig. 5 Comparison of computed shear wave velocity values with actual field data

Takada [27] (replicating a typical field deposit) are used in the analysis due to the absence of detailed soil information in Feng et al. [8], thereby yielding slightly varying result in the present study. However, both the soil types selected represent heterogeneous granular soil types encountered in the field, and thus the validation is justified within the limits of numerical and experimental accuracy.

Further, as can be observed from Fig. 5, the V_s values obtained in the present study increases from 150 m/sec to 250 m/sec at a depth of 2 m, thereby indicating an improvement in the order of 66% due to DC. In this regard, it is important to take into consideration the structural requirements from improved ground based on shear wave profile data obtained during subsoil investigation. The criteria outlined by the National Earthquake Hazards Reduction Program (NEHRP) [30, 31] for classification of site categories is presented in Table 2, based on the shear wave velocity measured in top 30 m of soil (V_s^{30}), which respond critically to ground shaking. As evident from the tabulated data, the V_s values obtained in the improved ground in the present study comply to the characteristics of stiff soil ($180 \leq V_s^{30} \leq 360$ m/sec) suitable for foundation support, which is a significant improvement over the values obtained initially in the untreated ground, classifying it as a soft soil type ($V_s^{30} < 180$ m/sec) susceptible to compression on loading.

Parametric Studies on DC

Effect of Energy Imparted

The procedure of DC involves impact of tamper mass on the soil surface, thereby transferring kinetic energy to the soil. Hence, energy per blow of impact is considered as a

Table 2 Site classifications based on recorded shear velocity in the field

Class ^a	Average shear wave velocity, V_s^{30} (m/sec) ^b	Soil type
A	$V_s^{30} > 1500$	Hard rock
B	$760 \leq V_s^{30} \leq 1500$	Rock
C	$360 \leq V_s^{30} \leq 760$	Very dense soil/soft rock
D	$180 \leq V_s^{30} \leq 360$	Stiff soil
E	$V_s^{30} < 180$	Soft soil [PI > 20]
F	$V_s^{30} < 180$	Special soils requiring site-specific evaluation [PI > 75]

^aAccording to site categories proposed by the National Earthquake Hazards Reduction Program (NEHRP) [30, 31]

^bShear wave velocity measured in top 30 m of soil [responding critically to ground shaking]

very crucial design factor in DC. However Oshima and Takada [27] and Lee and Gu [32] have reported that momentum also plays an important role in deciding the efficiency of DC. Hence, while conducting parametric studies related to various parameters of DC, the effect of energy and momentum are studied relative to each other as constant.

In order to study the effect of energy imparted, two sets of numerical analysis are done, as presented in Fig. 6a, the first five with constant momentum of 198.1 t.m/sec, and next three tests with constant momentum of 396.2 t.m/sec, all close to real-life field conditions. Similar methodology was employed by Lee and Gu [32] for investigating the impact of energy and momentum of DC on dry sands, wherein the momentum values selected were in the range of (200–400) t.m/sec. In the present study, in case of the first five tests, the energy levels are selected as 141.4, 173.3, 223.6, 200 and 245 t.m, whereas, in the second set, corresponding energies are 282.9, 346.4 and 400 t.m. The variation of V_s with depth (D) shown in Fig. 6a depicts the fact that, for a constant momentum but increasing energy, there occurs very little increase in V_s along the depth of soil, and the depth of improvement is almost constant. Further, it can also be observed that with an increase in momentum from 198.1 to 396.2 t.m/sec, the V_s profile increases, along with an increase in the corresponding depth of improvement. Hence, it can be inferred that the energy imparted during impact has comparatively lesser impact on the improvement due to DC.

Effect of Momentum

In order to investigate the impact of momentum on DC, two sets of experiments are performed with constant energy levels of 200 t.m (corresponding momentum values: 198.1, 280.1, 177.2, 242.6 and 313.2 t.m/sec) and 400 t.m. (corresponding momentum values: 396.2, 323.5 and 442.9 t.m/sec) as shown in Fig. 6b, thereby

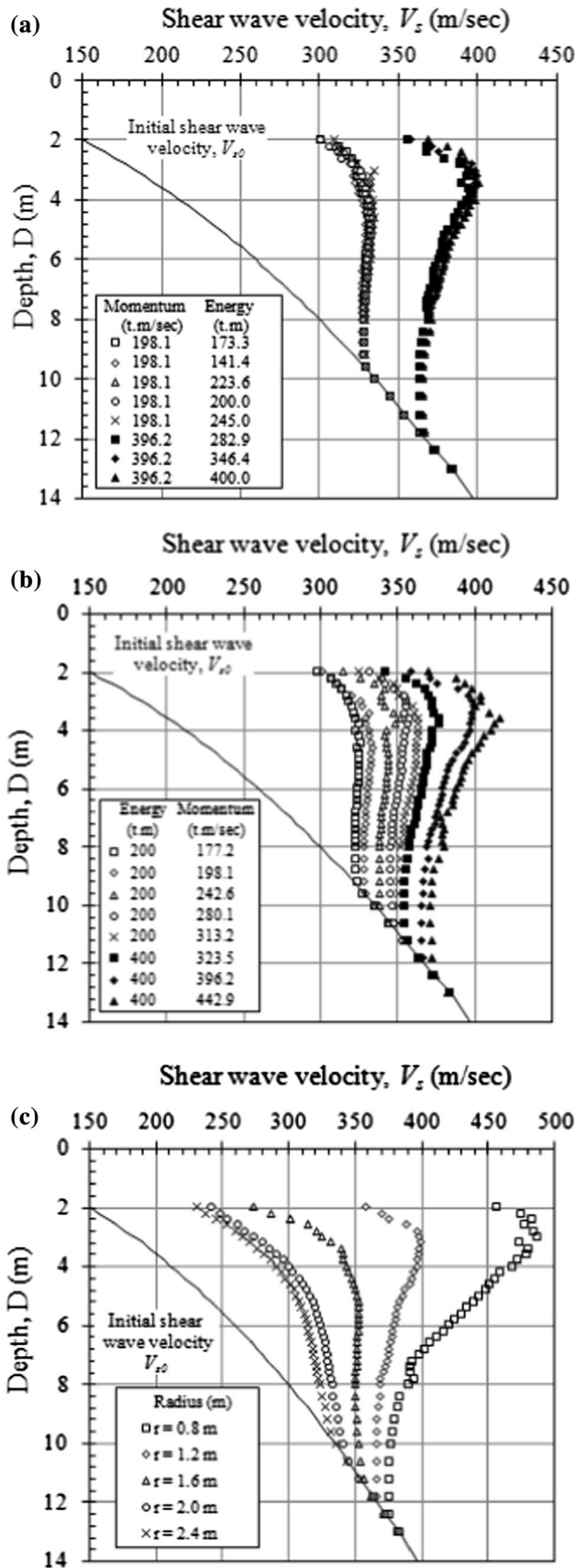
representing values adopted typically in field. Over the range of momentum examined, it is evident from the variation of V_s with depth presented in Fig. 6b, that both the shear wave velocity (V_s) and depth of improvement increase significantly (by almost 40%) with increase in momentum. Hence, it can be concluded that the degree and depth of improvement after DC in terms of shear wave profiling is effected predominately by momentum and not energy of tamper. The above observation is consistent with the findings of Lee and Gu [32] in terms of relative density increase after DC.

Effect of Tamper Radius

The effect of radius of tamper is investigated using five different radius, viz. 0.8, 1.2, 1.6, 2.0 and 2.4 m, maintaining the energy and momentum of tamper as 400 t.m and 396.2 t.m/sec respectively. The values of tamper radius selected in the present case represent magnitudes adopted frequently in the field. The corresponding shear wave profile is presented in Fig. 6c, plotted at a distance of 2 times the respective radius. It can be observed from Fig. 6c, that the V_s profile decreases all along the depth of soil with increase in radius (by almost 60%), which may be attributed to the fact that, with increase in radius, the momentum and energy per unit area reduces. Further, it can also be observed that depth of improvement reduces with increase in radius for constant energy and momentum.

Quantification of Soil Improvement in Terms of V_s

The above discussion involving the effect of different design parameters related to DC on soil improvement is qualitative in nature. To extend these observations for direct application in field during execution of DC, the results need to be generalized and quantified. In order to achieve this, the results on the effect of momentum and radius are normalised and plotted in Fig. 7a, b, as these two



◀Fig. 6 Shear wave velocity profiling with depth after DC. a Effect of energy imparted. b Effect of momentum. c Effect of radius

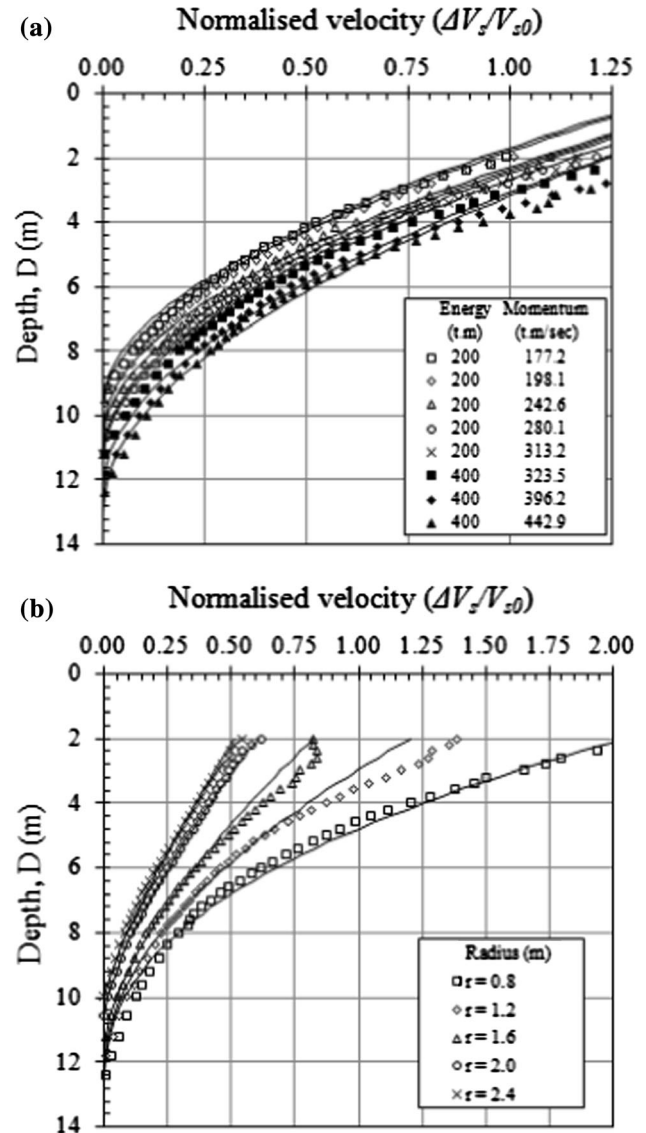


Fig. 7 Normalized shear wave velocity profile with depth. a Effect of momentum. b Effect of radius

parameters have been identified previously to play a major role in regulating the degree and depth of improvement. The increase in shear wave velocity (ΔV_s) is normalised against initial magnitude of shear wave velocity (V_{s0}) recorded before DC, so that the normalised result ($\Delta V_s/V_{s0}$) is applicable to various soil types exhibiting different values of initial shear wave velocity. Effect of energy on ΔV_s as already shown is negligible, so it is omitted for further analysis. It can be observed from Fig. 7a, b, that results of all the numerical simulations involving various radius and

momentum combinations corresponding to particular tamper energies show a similar trend. If D is assumed to represent the depth of soil from surface and $f(D)$ is a function representing the variation of normalised shear wave velocity ($\Delta V_s/V_{s0}$), then two observations can be made for the numerical tests simulated. Firstly, $f'(D)$ is almost zero at a depth which can be considered as the depth of improvement (d). Secondly, $f'(D)$ increases with decrease in depth. Both these observations are satisfied by Eq. (8):

$$\frac{\Delta V_s}{V_{s0}} = f(D) = \left(\frac{d - D}{m}\right)^n \tag{8}$$

By using Eq. (8), all the curves presented in Fig. 7a, b are fitted to suitable regression equations using three variables d , m and n to arrive at design charts for direct application in field. It can be observed that, all the curves are represented quite accurately by Eq. (8) except at few regions where conservative values have been adopted for curve fitting. The design parameters from Fig. 7a, b, are plotted in Fig. 8a, b, in order to observe the dependence of the parameters d , m and n on momentum (M) and radius (r). Equations (9a–9c) represent the dependence of the parameters d , m and n very accurately as seen in Fig. 8a, b.

$$d = 0.0121M - 1.825r + 9.5 \tag{9a}$$

$$m = 0.0059M + 3.95r + 2.05 \tag{9b}$$

$$n = -0.7125r + 2.81 \tag{9c}$$

In this case, it can be observed that parameters d and m are dependent on both momentum and radius but n is dependent exclusively on the tamper radius. In this connection, it should be mentioned that Eqs. (9a–9c) are derived based on momentum values ranging from (175–450) t.m/sec, energy values lying in the order of (175–400) t.m and tamper radius ranging from 0.8 to 2.4 m. The values hereby presented in connection with upper and lower ranges of energy, momentum and tamper radius closely resemble that applied in the field during DC on loose granular deposits.

Proposed Method for Estimating Improvement Along Soil Depth

Based on the findings and equations presented above, a method is proposed for estimating the shear wave velocity profile after DC along the depth of soil. The method differs from most of the existing methods listed in literature in a sense that, in this case, the variation of V_s is plotted along the entire soil depth, and not at a single point, thereby giving a clear picture of the soil improvement after DC. Initially, Eqs. (9a–9c) should be used to predict the design parameters d , m and n using the values of momentum (M) imparted in field and radius (r) of tamper being used. The shear wave velocity profile after DC can be

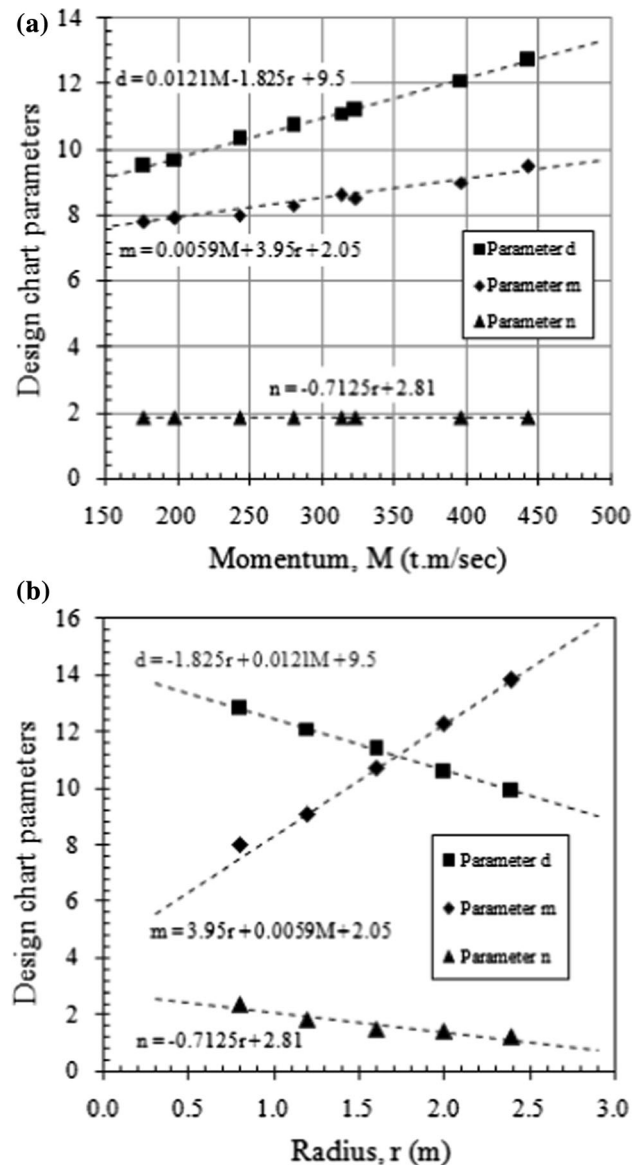


Fig. 8 Determination of design chart parameters. a Effect of momentum. b Effect of tamper radius

subsequently derived by using Eq. (8). The above process needs to be repeated for various combinations of momentum and tamper radius in order to achieve the required magnitude of V_s after DC, following which the corresponding mass, height and radius of tamper can be used in field to achieve the desired degree and depth of improvement.

Conclusions

The paper presents results of a numerical model study for predicting the degree and depth of improvement in the field due to dynamic compaction on soil by means of shear wave

velocity profiling. An elasto-plastic model with Drucker–Prager failure criteria is incorporated in the present study using FE software ABAQUS, and the response of the soil to excessive deformations induced by dynamic impact is incorporated by adopting an updated Lagrangian large-strain formulation. The effect of multiple tamper drops on loose dry sand is investigated numerically, and validated with the results of a centrifuge model test, and numerical analyses published in literature. The shear wave velocity of soil samples is assessed numerically based on the value of shear modulus, and the improvement in soil strength post DC is evaluated in terms of shear wave velocity profiling by varying the various design parameters (e.g. tamper radius, energy, momentum) related to DC. Based on the analysis and interpretation of results, the following conclusions can be drawn:

1. The degree and depth of improvement in the original loose granular soil increases by 66% due to dynamic impact as per the study based on shear wave profiling data, thereby indicating the effectiveness of DC. The above finding facilitates construction of shallow foundations in sites exhibiting poor subsoil profiles by means of DC, thereby economizing the project and maintaining sustainability in construction by avoiding high carbon footprints associated with expensive deep foundations.
2. An increase in momentum is found to result in 40% increase of the improvement depth, whereas, energy imparted has comparatively lesser impact on improvement. Further, a decrease in tamper radius results in higher depth of improvement (about 60%) for a constant energy and momentum.
3. A design method is eventually proposed in the present paper to estimate the soil improvement in field after DC in terms of shear wave velocity (V_s) profiling. The proposed method incorporates the effect of momentum and tamper radius, including the initial state of the soil existing in field in terms of V_s . Further, the results have been normalized and generalized to take into account the effect of various soil type exhibiting different values of initial shear wave velocity (V_{s0}). The design method outlined in the present study is thus useful for deciding the momentum of impact, and the tamper radius to be adopted in the field for achieving prefixed (target) depth and degree of improvement of soils based on shear wave profiling data. The above technique is advantageous as compared to methods proposed by earlier researchers, in a sense that, in this case, the in situ state of soil, as well as the degree and extent of improvement can be quantified along the entire depth of soil, contrary to earlier assumptions of a constant value throughout the depth.
4. In this regard, it should be mentioned that, the conclusions drawn on the effect of energy, momentum and tamper radius are based on a particular soil type (dry granular material), and should be extended for different soil conditions existing in field. Further, the results are plotted at a distance of two times the radius from tamper center for a single footprint. In general, the improvement will be more than the results presented because of overlapping effect contributed by different footprints, thereby rendering the results of the present study on the conservative side. Moreover, the study can be further extended in future by adopting higher energy levels and heavier tamper masses to ensure a greater depth and extent of improvement than that reported in this context. Further, the method proposed in the present analysis needs extensive field validation for accurate prediction of soil improvement, and further studies are warranted in this area.

References

1. Spaulding C, Masse F, LaBrozzi J (2008) Ground improvement technologies for a sustainable world. In: Proceedings of GeoCongress 2008: geosustainability and geohazard mitigation, Civil engineering magazine archive 78(4): 891–898
2. Menard L, Broise Y (1975) Theoretical and practical aspect of dynamic consolidation. *Géotechnique* 25(1):3–18
3. Leonards GA, Cutter WA, Holtz RD (1980) Dynamic compaction of granular soil. *J Geotech Eng* 106(1):35–44
4. Mayne PW, Jones JS, Dumas JC (1984) Ground response to dynamic compaction. *J Geotech Eng* 110(6):757–774
5. Kumar S, Puri VK (2001) Soil improvement using heavy tamping—a case history. *ISIT J Earthq Technol* 38(2–4):123–133
6. Zou WL, Wang Z, Yao ZF (2005) Effect of dynamic compaction on placement of high-road embankment. *J Perform Constr Facil* 19(4):316–323
7. Bo MW, Na YM, Arulrajah A, Chang MF (2009) Densification of granular soil by dynamic compaction. *Ground Improv* 162(3):121–132
8. Feng SJ, Shui WH, Tan K, Gao LY, He LJ (2011) Field evaluation of dynamic compaction on granular deposits. *J Perform Constr Facil* 25(3):241–249
9. Feng TW, Chen KH, Su YT, Shi YC (2000) Laboratory investigation of efficiency of conical-based pounders for dynamic compaction. *Géotechnique* 50(6):667–674
10. Arslan H, Baykal G, Ertas O (2007) Influence of tamper weight shape on dynamic compaction. *Ground Improv* 11(2):61–66
11. Hajjalilue-Bonab M, Rezaei AH (2009) Physical modelling of low-energy dynamic compaction. *Int J Phys Modell Geotech* 9(3):21–32
12. Bonab MH, Zare FS (2014) Investigation on tamping spacing in dynamic compaction using model tests. *Ground Improv* 167(3):219–231
13. Kundu S, Viswanadham BVS (2015) Studies to evaluate the impact of tamper on the depth of improvement in dynamic compaction. *Jpn Geotech Soc Spec Publ* 2(59):2033–2037

14. Taylor RN (1995) Centrifuges in modelling: principles and scale effects. In: Taylor RN (ed) *Geotechnical centrifuge technology*. Blackie Academic and Professional, Glasgow
15. Scott RA, Pearce RW (1975) Soil compaction by impact. *Géotechnique* 25(1):19–30
16. Holeyman A (1985) Unidimensional modellization of dynamic footing behavior. In: *Proceedings of the 11th conference on soil mechanics and foundation engineering*, San Francisco, Vol 2. Balkema, Rotterdam, pp 761–764
17. Smits M, de Quelerij L (1989) The effect of dynamic compaction on dry granular soils. In: de Janeiro R (ed) *Proceedings of the 12th international conference on soil mechanics and foundation engineering*, Vol 2. Taylor & Francis, Routledge, pp 1419–1422
18. Chow YK, Youg DM, Yong KY, Lee SL (1992) Dynamic compaction analysis. *J Geotech Eng* 118(8):1141–1157
19. Chow YK, Youg DM, Yong KY, Lee SL (1992) Dynamic compaction of loose sand deposits. *Soils Found* 32(4):93–106
20. Chow YK, Youg DM, Yong KY, Lee SL (1994) Dynamic compaction of loose granular soils: effect of print spacing. *J Geotech Eng* 120(7):1115–1133
21. Corapcioglu MY, Mathur S, Bear J (1993) Dynamic compaction of saturated porous columns. *J Eng Mech* 119(8):1558–1578
22. Gunaratne M, Ranganath M, Thilakasiri S, Mullins G, Stinnette P, Kuo C (1996) Study of pore pressures induced in laboratory dynamic consolidation. *Comput Geotech* 18(2):127–143
23. Pan JL, Selby AR (2002) Simulation of dynamic compaction of loose granular soils. *Adv Eng Softw* 33(7–10):631–640
24. Gu Q, Lee FH (2002) Ground response to dynamic compaction of dry sand. *Géotechnique* 52(7):481–493
25. Ghassemi A, Pak A, Shahir H (2009) Validity of Menard relation in dynamic compaction operations. *Ground Improv* 162(1):37–45
26. Nashed R, Thevanayagan S, Martin GR (2009) Dynamic compaction of saturated sands and silty sands: design. *Ground Improv* 162(2):81–92
27. Oshima A, Takada N (1998) Evaluation of compacted area of heavy tamping by cone point resistance. In: Kimura T, Kusakabe O, Takemura J (eds) *Proceedings of the Centrifuge'98*, Tokyo, Vol 1. Balkema, Rotterdam, pp 813–818
28. Zerwer A, Cascante G, Hutchinson J (2002) Parameter Estimation in Finite Element Simulations of Rayleigh Waves. *J Geotech Geoenviron Eng* 128(3):250–261
29. Dimaggio FL, Sandler IS (1971) Material models for granular soils. *J Eng Mech Div* 97(3):935–950
30. Mohamed AME, Abu El Ata ASA, Azim FA, Taha MA (2013) Site specific shear wave velocity investigation for geotechnical engineering applications using seismic refraction and 2D multi-channel analysis of surface waves. *NRIAG J Astron Geophys* 2(1):88–101
31. NEHRP (2010) NEHRP recommended seismic provisions for new buildings and other structures (FEMA P-750). Building Seismic Safety Council, National Institute of Building Sciences, Washington
32. Lee FH, Gu Q (2004) Method for estimating dynamic compaction effect on sand. *J Geotech Geoenviron Eng* 130(2):139–152